Friction in (im-)miscible polymer brush systems and the role of transverse polymer-tilting

Sissi de Beer[†,‡] and Martin H. Müser[∗,†,¶]

Jülich Supercomputing Centre, Institute for Advanced Simulation, Forschungszentrum Jülich, Jülich, Germany

E-mail: m.mueser@fz-juelich.de

Abstract

It was found recently that two polymer brushes in a tribological contact do not interdigitate when each polymer brush has its own preferred solvent, leading to low friction and low wear rates. Here, we demonstrate, using molecular dynamics simulations, that mutually miscible and fully solvated brush systems do not significantly overlap either if the radii of curvature of the surfaces, to which the brushes are grafted, are sufficiently small. The brushes achieve this by bending away from the center of the contact, while they bend toward the center of the capillary when being only partially solvated. For the fully solvated brushes, immiscible systems also show smaller friction than miscible systems, although the friction reduction is less than for partially solvated brushes.

[∗]To whom correspondence should be addressed
[†]Jülich Supercomputing Centre, Institute for Advanced Simulation, Forschungszentrum Jülich, Jülich, Germany
[‡]Materials Science and Technology of Polymers, MESA+ Institute for Nanotechnology, University of Twente, P.O. Box 217, 7500 AE Enschede, The Netherlands
[¶]Dept. of Materials Science and Engineering, Universität des Saarlandes, Saarbrücken, Germany

Introduction

Biological lubricants, as found, e.g., in human joints or on the skin of snails, are very efficient in maintaining low friction during sliding motion. Nature attains such efficient lubrication via hydrophilic sugar chains that attach to surfaces and protein backbones.[1] The sugar chains keep a water-based, low-viscosity liquid within the contact between surfaces, resulting in friction coefficients lower than 0.02[2] even for local pressures up to 50 atmospheres.[3] By end-anchoring polymers at a high density to solid surfaces, one can mimic such biological lubricants:[4,5] the grafted polymers swell in a good solvent and keep the low-viscosity liquid in the contact as long as the externally applied pressure is lower than the osmotic pressure in the solvent.[6] Besides potentially serving as efficient lubricants, solvated polymer brushes also hold great potential for application in smart materials,[7] bio-engineering[8] and oil recovery.[9]

An essential disadvantage, withholding industry from applying polymer brushes as lubricants, has been that polymers on opposing surfaces can interpenetrate.[10–12] The latter can cause high friction and wear due to chain scission and pull-out.[13–15] Early molecular dynamics (MD) simulations, which allowed for visualising the polymer-segments in brushes, revealed a clear inter-brush overlap[16] that correlates with the frictional response upon relative sliding of opposing brushes.[17,18] Shear stress on the interdigitated polymers stretches and tilts them, which induces a reduction of the overlap zone with increasing velocity. For this reason sheared polymer brushes display shear-thinning,[17,18] which has been shown to result in a sub-linear friction velocity relation $F \sim v^{\kappa}$,[19,20] with $\kappa = 0.54 - 0.57$.[19–21] Experimentally, it was recognized that interdigitation and friction between two charged polymer brushes can be tuned by applying an electric field.[22] Moreover, we have recently shown that interdigitation between polymers on opposing surfaces can even be completely circumvented by applying solvent-induced immiscible polymer brush systems.[23] The friction for these systems was found to be two orders of magnitude lower than for miscible polymer brush systems.

While for the parallel plate geometry, interdigitation was found to be the main source of dissipation in sliding opposing polymer brushes,[17–21] it was recently shown that alternative dissipation

mechanisms can come into play for brush-bearing engineering surfaces .[24] Engineering surfaces have a roughness distribution over many length-scales.[25] Consequently, asperities on the opposing surfaces can collide, inducing solvent-squeeze-out and re-absorption,[26] shape hysteresis,[27] transient interdigitation[28] and, in partially solvated contacts, capillary hysteresis.[29] The latter is most likely to dominate friction between partially solvated miscible polymer brush systems for small velocities.[24]

In this article we elaborate on the MD simulations presented in Refs 23 and 24 and show that interdigitation can be insignificant for solvent-immersed polymer brushes on curved surfaces too. When the radius of curvature of the brush-bearing surfaces is small enough, the polymers bend to escape out of the contact, as was observed before for brushes on nano-particles that are placed at close distance.[30] In contrast, for partially solvated brushes, the polymers at the edge of the contact bend in the inward direction, because the surface tension of the solvent bundles the polymers together. We discuss the frictional response to sliding and the shear-thinning exponents of both solvation-methods and compare them to the friction between dry brushes in relative sliding motion. Moreover, we systematically vary the miscibility of the different system-components and study its effect on the friction coefficient.

Model and Methods

For the simulations we set up two cylinders (radius $R = 100\sigma$, see Figure 1) that each bear 950 end-anchored polymers at a grafting density α of approximately 3x the critical grafting density $\alpha_c = 1/(\pi R_{gyr}^2)$ for brush formation.[31,32] Each polymer consists of $N = 30$ beads (test runs using $N = 100$ beads showed qualitatively similar results). The walls consist of a single layer of surface-atoms (fcc [111] with a lattice constant of 1.2σ). The wall atoms are connected to their lattice sites with harmonic springs ($k = 32\varepsilon/\sigma^2$) and to each other using anharmonic springs ($k = 30\varepsilon/\sigma^2$). The latter ensures a maximum displacement of the wall atoms by 0.4 σ. For the simulations we employ an explicit solvent that consists out of dimers. We choose solvent-dimers instead of

solvent-monomers, because the former reduce artificial results due to layering close to the walls.[19] Due to the cylindrical shape of the wall, we have a smooth transition to a region where the brushes are not in contact. By simulating a contact between two cylinders we approximate the contact between two asperities, such as found on realistic engineering surfaces, more closely than for the parallel plate geometry. For brushes grafted from curved surfaces, the density profiles can deviate from those at flat surfaces.[33] However, our ratio of N over R is sufficiently small that these effects are unnoticeable.[34]
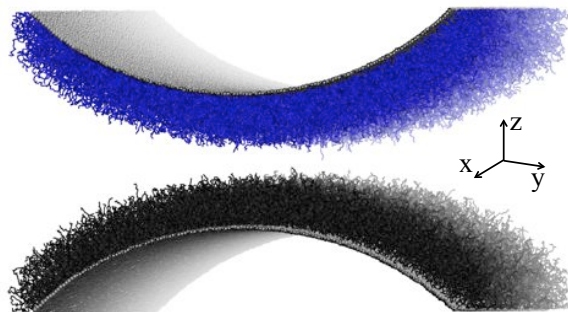
Figure 1: Snapshot of our simulation cell showing the two polymer-bearing cylinders. (snapshot was rendered using VMD[35])

Our simulations are based on the generic Kremer-Grest model,[36] which qualitatively reproduces the physical behavior of end-anchored[12] and surface-adsorbed[37] polymers as well as polymer melts.[38] The Kremer-Grest model consists of elastic springs between consecutive beads, imposed by the FENE potential,

$$V_{\text{FENE}} = \frac{1}{2}kR_0^2\ln\left[1 - \left(\frac{r_{ij}}{R_0}\right)^2\right],\tag{1}$$

using a stiffness $k = 30\varepsilon/\sigma^2$ and a maximum extension $R_0 = 1.5\sigma$. The excluded volume effects at short distances and the long-ranged van der Waals interaction are described by the Lennard Jones (LJ) potential with the functional form

$$V_{\text{LJ}}(r_{ij}) = 4\varepsilon_{ij}\left[\left(\frac{\sigma_{ij}}{r_{ij}}\right)^{12} - \left(\frac{\sigma_{ij}}{r_{ij}}\right)^{6}\right],\tag{2}$$

4

where r_{ij} is the distance between two interacting beads. Typical values for the pair-dependent parameters ε_{ij} and σ_{ij} are $\varepsilon = 30$ meV and $\sigma = 0.5$ nm,[39] respectively, which we use as units for energy and length. The beads represent Kuhn units of typically $3-5$ monomers. Therefore, the unit of mass is $m = 10^{-22}$ kg and the unit of velocity is $v = 7$ m/s. For the interaction-parameters we distinguish between non-connected and connected, consecutive beads. The LJ interaction between consecutive beads is purely repulsive ($\varepsilon_{pp} = 1$, $\sigma_{pp} = 1$ and $r_{cut} = 2^{1/6}\sigma_{pp}$). Non-consecutive polymer beads interact with the same ε and σ as consecutive beads, except that we use a cut-off of $1.6\,\sigma$, such that the polymers are slightly attractive. For non-connected solvent-beads the LJ parameters are $\varepsilon_{ss} = 0.5$, $\sigma_{ss} = 1$ and $r_{cut} = 2.5\sigma_{ss}$. For these parameters the dimers are in the liquid phase over the entire range of pressures used in the simulations ($P = 0 - 25\varepsilon/\sigma^3$). The LJ parameters for the interaction between solvent and polymer are $\varepsilon_{ps} = 1.2$, $\sigma_{ps} = 1$ and $r_{cut} = 2.5\sigma_{ps}$. These LJ parameters result in good solvent conditions and miscibility. The interaction between the wall-atoms and the polymers is purely repulsive ($r_{cut} = 2^{1/6}\sigma_{pw}$) such that we would have the classical mushroom-brush transition at α_c.[40] The interaction between the solvent-beads and the wall-atoms is slightly attractive ($\varepsilon_{sw} = 0.6$, $\sigma_{sw} = 1.3$ and $r_{cut} = 1.6\sigma_{sw}$), which would result in a contact angle of around 10° for the solvent on a bare surface.[41] Opposing polymers (P and $\bar{P}$), different solvents (S and $\bar{S}$) and polymers with one of the solvents (P and $\bar{S}$ / $\bar{P}$ and S) are made immiscible by shifting the cut-off to the potential minimum; $r_{cut} = 2^{1/6}\sigma_{ij}$.

To impose sliding motion, we move the lattice sites of both surfaces in opposite directions, with constant velocities v and $-v$ in x. Periodic boundary conditions are applied in x and y. Newton's equations of motion are solved with the velocity Verlet algorithm, as implemented in LAMMPS,[42] using a time step of $0.005\,\sigma\sqrt{m/\varepsilon}$. The simulations are performed in the NVT ensemble (temperature $T = 0.6\varepsilon/k_B$) using a Langevin thermostat (time-constant $\tau = 1.0\sigma\sqrt{m/\varepsilon}$) that only acts on the wall-atoms. The thermostat is switched off in the normal direction z and shear direction x such that there is no measurable effect of the thermostat on the hydrodynamic response of the brushes.[43]

Results and discussion

Solvent-immersed systems
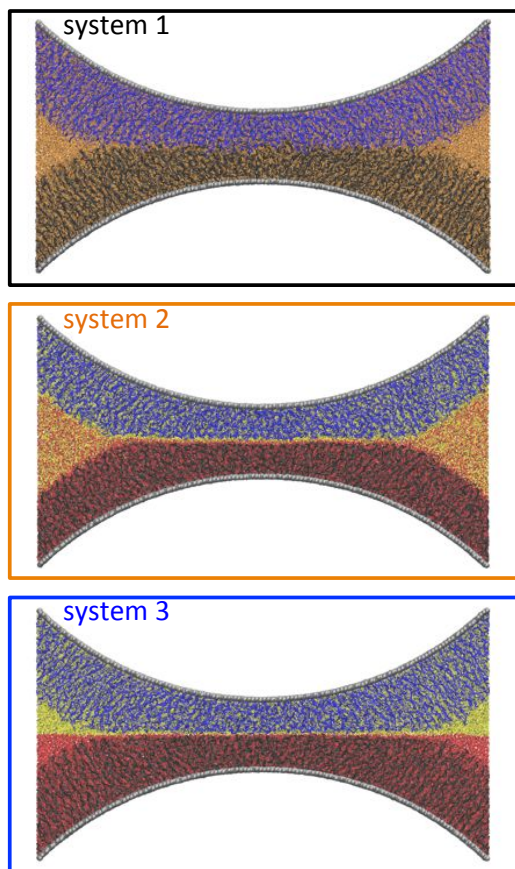
Figure 2: The 3 different types of solvent-induced (im-)miscibility studied in this article (see also Table 1). The systems consist of two different types of polymers P (black) and $\overline{P}$ (blue) and for system 1 a single solvent S (orange) or for systems 2 and 3 two different solvents S (red) and $\overline{S}$ (yellow). For system 1 all components are miscible. For system 2, P and $\overline{S}$ are immiscible and also $\overline{P}$ and S are immiscible, such that there is a preferred absorbance of each solvent in one of the brushes, while all other combinations, including S and $\overline{S}$, mix. System 3 is the same as system 2 except that now S and $\overline{S}$ are also immiscible.

To study the effect of different types of (im-)miscibility on the friction for systems that are fully immersed in solvent, we set up 3 different systems, as shown in Figure 2. The systems consist of a surface bearing polymer P and an opposing surface bearing polymer $\overline{P}$. The simulation box is filled up with solvent S (system 1) or solvents S and $\overline{S}$ (systems 2 and 3). To compare the different

Table 1: The relative interaction for polymers P and $\overline{\text{P}}$ and solvents S and $\overline{\text{S}}$ resulting in the three types of system-(im-)miscibility. Plus sign indicates attractive interactions and miscibility, while a minus sign indicates repulsive interactions and immiscibility

system	PS,$\overline{\text{PS}}$	$\overline{\text{P}}$S / P$\overline{\text{S}}$	$\overline{\text{S}}$
1	+	+	+
2	+	-	+
3	+	-	-

systems, we adjusted the distance between the cylinders such that the equilibrium normal force is approximately $F_{\text{N}} = 20,000\varepsilon/\sigma$, which translates to a pressure $P = 100$ MPa in the central slab (of width 15 σ) of the contact. In this central region the force per unit area is approximately constant, while it decreases to zero towards the edge of the contact. We keep the number density of the solvent in the bulk region outside the brushes constant at 0.87 (which is the average density of bulk solvent at $P = 1\sigma^3/\varepsilon$ and $T = 0.6\varepsilon/k_{\text{B}}$). The interactions between the different system components polymer P, polymer $\overline{\text{P}}$, solvent S and solvent $\overline{\text{S}}$ are given in Table 1. A plus sign denotes attractive interactions as described in the Model and Methods section, while a minus sign indicates that the cut-off of the potential was set to $r_{\text{cut}} = 2^{1/6}\sigma_{ij}$ rendering the components immiscible.

In system 1 all components mix such that there is a single-phase solvent that absorbs in both brushes (no preferred absorbance). Consequently the polymers from the opposing brushes interdigitate. However, as becomes apparent in Figure 3, interdigitation only occurs in the central region of the contact. Near the edges of the contact, the polymers bend in the outward directions instead of moving in the opposing brush, as observed earlier for brush-coated nano-particles in close contact.[30] The average transverse tilting angle (deviation from the surface normal) of all polymers in the depicted system is 23º in the outward direction. This outward bending is caused by the elastic deformation of the brushes and by the attractive polymer-solvent interactions. The transverse tilting angle depends on the curvature of the walls. For $R \to \infty$, as in the parallel plate geometry, there is no transverse tilting and thus interdigitation is high. For small R, the outward tilting is strong and interdigitation minimal, which is consistent with the observation that interdigitation between colliding star polymers is small.[27] This outward tilting of the polymers also implies that the effect of interdigitation on the friction for immersed brushes on engineering surfaces, which show a

7

roughness distribution on many length scales,[25] should be less than predicted from simulations in the parallel plate geometry. In a typical AFM measurement setup the ratio of brush height (typically 500 nm) over radius of curvature (approximately 5 μm) is 1/10 and thus comparable to the ratio used in our simulations. In the SFA, the curvature of the sample surfaces is much larger (5 cm), which means that the brush height over radius of curvature ratio is much smaller. Therefore, transverse polymer tilting will be of minor importance for SFA experiments.
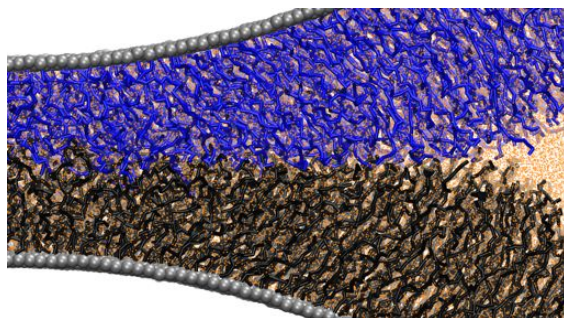
Figure 3: Zoomed in snapshot of system 1 of Figure 2 showing the transverse polymer tilting in the outward direction. In the central contact polymers initerdigitate. However, near the edge of the contact, we observe transverse polymer tilting. Those polymers prefer to bend out of the contact due to the elastic deformation and preferred interactions with the solvent in the bulk region.

One might think that the transverse tilting of the polymers also implies that the friction between sliding polymer brushes on rough surfaces will be lower than the friction for brushes on flat surfaces. However, in reality it is often observed that the friction for rough brush-bearing surfaces is higher than for flat surfaces.[44,45] This higher friction is caused by asperity collisions that occur during sliding the brushes that are attached to rough surfaces. During these asperity collisions, alternative dissipation mechanisms, such as shape hysteresis,[46] transient interdigitation,[28] solvent squeeze-out, and re-absorption,[26] can come into play.[24] Consequently, the friction between colliding, brush-bearing asperities can get relatively high. For the simulations in the present article we only slide in the lateral direction (parallel to the cylinder axes). Therefore, the above mentioned alternative dissipation mechanisms cannot affect our frictional response.

In system 2 the brushes are solvated with a 50-50 binary liquid mixture that consists of solvents S and $\overline{\text{S}}$. Polymers in binary solvent mixtures can show many peculiar effects,[47] such as a

co-nonsolvency-induced phase transitions[48,49] depending on the relative solvent quality and the relative solvent concentration. For our system solvent S is a good solvent for polymers P and a poor solvent for polymers $\overline{P}$. For the second solvent $\overline{S}$ the interactions are opposite: $\overline{S}$ is a good solvent for polymers $\overline{P}$ and a poor solvent for polymers P. Both solvents are perfectly miscible, while the polymer-solvent interactions between PS and $\overline{PS}$ are stronger than the interaction between the two solvents. Under our chosen circumstances, only the good solvent absorbs into the brush.[50] Due to the preferred absorbance of the solvents in their own brushes, there is almost no overlap between the brushes, as can be perceived from the sharp interface between the brushes of system 2 in Figure 2. As Figure 2 also shows, the apparent free brush height in system 2 is a bit lower than the brush heights of system 1 and 3. This effect has been attributed to a larger energy penalty for polymer fluctuations into the bulk solvent.[51] Moreover, the average transverse tilting angle is 17$^\text{o}$, which is 6$^\text{o}$ less than the tilting angle in system 1. This reduced transverse tilting of the polymers in system 2 compared to system 1 is due to the same energy penalty that circumvents polymers to move into the mixed bulk solvent.

For system 3 the interactions are the same as in system 2 except that in system 3 the 50-50 binary liquid mixture of solvents S and $\overline{S}$ does not mix. Consequently there is a sharp interface between the top and the bottom part of the simulation cell. Since there is no energy penalty for polymers to move into the bulk liquid, the average transverse tilting angle is 25$^\text{o}$, which is 8$^\text{o}$ larger than in system 2. Moreover, the transverse tilting angle is also larger than for system 1 (2$^\text{o}$), because interdigitation does not occur in system 3, which enhances the tendency of polymers to move out of the contact.

Figure 4 shows the friction coefficient μ versus velocity extracted from non-equilibrium simulations in which we slide systems 1-3 depicted in Figure 2. The friction coefficient is defined as the total friction force divided by the total normal force on the surfaces. As expected, for system 1, where the polymers interdigitate in the central region of the contact, we observe the highest friction coefficients. Upon fitting the data to the power-law relation $\mu = v^\kappa$, we find a shear-thinning exponent of $\kappa = 0.67$. The exponent is larger than the exponent of $\kappa = 0.53 - 0.57$ generally ob-
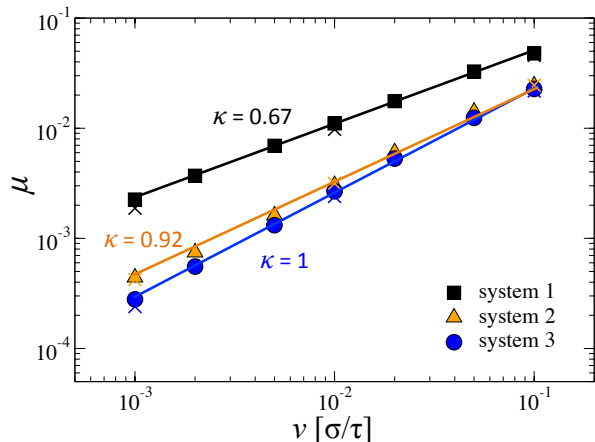
Figure 4: Friction coefficient μ versus velocity v upon shearing system 1 (black squares, fully miscible, no preferred absorbance), 2 (orange triangles, miscible solvents, preferred absorbance) and 3 (blue circles, immiscible solvents, preferred absorbance). The colored crosses denote μ for the same systems, but with immiscible polymers instead of the default miscible polymers employed in systems 1-3. The straight lines are fits to the power law relation $\mu = v^{\kappa}$.

served for sliding interdigitated polymer brushes.[19–21] The larger exponent might be caused by the curved surfaces, which causes the outward transverse tilting of the polymers such that the brushes are not everywhere strongly compressed and interdigitated. Another explanation for the higher exponent might be that the higher polymer density in the central contact region results in effectively dry brush friction.[19] A similar shear-thinning exponent ($\kappa = 0.69$) has been observed for sliding charged polymer brushes,[52] which was attributed to collective polymer / solvent motion resulting in effectively dry brush scaling.[19]

At the smallest velocities, the friction in systems 2 and 3 is approximately 10x lower than in the miscible system 1 (see Figure 4). The reduced friction in systems 2 and 3 is caused by the solvent-induced immiscibility due to the preferred absorbance of the two solvents in their own brushes, which prevents interdigitation. For system 3, where the two solvents do not mix, we find a linear relation between μ and v, while we observe a slight shear-thinning for system 2 ($\kappa = 0.92$). Analysis of the velocity profiles of the solvents and the simulation snapshots indicates that shear-thinning for system 2 is caused by an increase of the effective distance between the brushes with increasing velocity. The solvent's velocity gradient penetrates into the brushes, such

10

that the polymers shear-align. The polymer-alignment increases with velocity, such that the gap between the brushes increases with velocity and, thus, the shear stress decreases sublinearly with velocity.

The difference in friction between systems 2 and 3 continues to increase with decreasing velocity until system 2 reaches a linear response. At very small velocities, in the linear response regime, the difference in friction between systems 2 and 3 is caused by reduction in viscous drag force due to slip at the interface as found at the interface of two immiscible liquids.[53] Experimentally it was found that for single brushes that are swollen due to preferred absorbance in binary liquid mixtures, lubrication slightly deteriorates compared to single brushes in single-component good solvents.[54] Just like in our system 2, the edge of the brush is expected to be less 'fluffy' than for a brush solvated with a single-component good solvent, which can also slightly increase friction.

The crosses in Figure 4 denote the friction coefficients for system 1-3, where we made the interaction between all the polymers purely repulsive ($r_{cut} = 2^{1/6}\sigma_{pp}$) instead of slightly attractive ($r_{cut} = 1.6\sigma_{pp}$) as in our default systems. As becomes clear in Figure 4, the friction coefficients are only marginally affected by the polymer-polymer interactions. These results can be expected, since polymers in good solvents are effectively repulsive.

Solvent-undersaturated systems

While most AFM and SFA experiments are performed with solvent-immersed polymer brush systems,[4,22,45,54] in tribometer experiments the brushes are often undersaturated in solvent and/or in equilibrium with the gas-phase.[55] Moreover, full solvation cannot be always guaranteed in practical situations. To mimic such circumstances, we set up the same systems as depicted in Figure 2, except that most of the solvent is removed such that there is approximately one solvent bead per polymer bead. Judging from the effective brush height, these conditions are roughly comparable to polyelectrolyte brushes kept at a relative humidity of 90%.[56] The simulations of systems 1u-3u (u stands of undersaturated) are performed at the same distance of 10.9σ between the cylinder apices. At this distance, the normal load of system 3u is $F_N = 20,000\varepsilon/\sigma$, which is the same nor-

mal load as we chose for our solvent-immersed systems (although the local pressure can change by approximately 25% due to the change in contact area[21]).
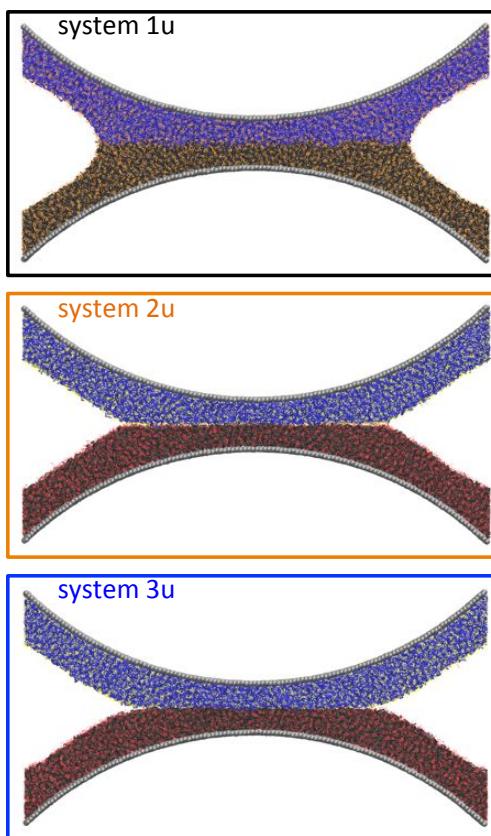
Figure 5: The same systems as in Figure 2, except that the systems are now undersaturated in solvent. For system 1u all components, polymers P (black) and $\overline{\text{P}}$ (blue) and solvent S (orange), are miscible. For system 2u, P and solvent $\overline{\text{S}}$ (yellow) are immiscible and also $\overline{\text{P}}$ and solvent S (red) are immiscible, such that there is a preferred absorbance of each solvent in one of the brushes, while S and $\overline{\text{S}}$ mix. System 3u is the same as system 2u except that now S and $\overline{\text{S}}$ are also immiscible.

In system 1u, where all components mix, a capillary is formed in the contact. The surface tension of the solvents bundles the interdigitated polymers together. Due to the capillary, the average transverse tilting angle of the polymers in the contact is a lot less than for the solvent-immersed system 1, namely 11° for system 1u compared to 23° for system 1. Despite, the distance between the cylinders apices being smaller than the distance in the immersed systems. As can be seen in Figure 6, the polymers only tilt in the outward transverse direction in a small region

between the centrum of the contact and the edge of the contact. In the central region the polymer do not tilt but interdigitate with the opposing brush. At the edge of the contact, polymers are stretched out closing the capillary at an angle parallel to the surface normal. Outside the contact the polymers show a slight inward tilting, which allows them to be part of the capillary.
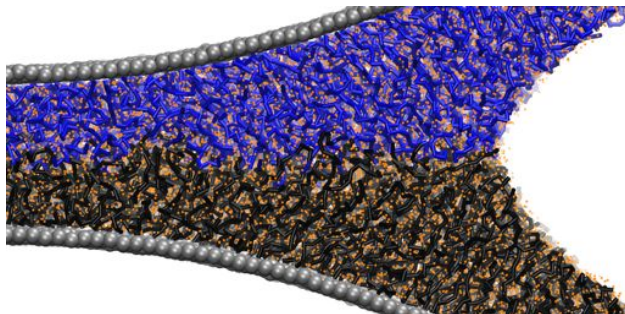
Figure 6: Zoomed in snapshot of system 1u of Figure 5 showing the bundling of the polymers in the contact due to the surface tension of the solvent. Moreover, there is on average a lot less transverse polymer tilting in the outward direction.

In system 2u, the two solvents S and $\overline{S}$ each prefer to be in their own polymer brush. However, S and $\overline{S}$ mix. Consequently there is a small capillary formed in the contact, solely due to the surface tension of the mixed solvents. The capillary causes a kink in the brush-shape at the edge of the contact. System 3u is the same system as system 2u except that solvent S and $\overline{S}$ do not mix. Therefore, there is no capillary formed in system 3u, such that the shape of the brushes smoothly evolves from inside to outside the contact. The average transverse tilting angle of the polymers of system 2u and 3u are 15° and 16°, respectively.

Figure 7 shows the friction coefficient μ for sliding system 1u-3u (depicted in Figure 5) for different velocities v. For the completely miscible system 1u, the friction coefficient depends on the velocity via a power law scaling $\mu = v^{\kappa}$, with shear-thinning exponent $\kappa = 0.55$. This exponent is consistent with the exponent of $\kappa = 0.53 - 0.57$ generally found for strongly compressed polymer brushes that are slid in the parallel plate geometry.[19–21] For system 2u, in which the solvents show a preferred absorbance but mix, interdigitation is again eliminated. Consequently, μ is at the smallest velocities around a factor 20 lower than for the miscible system 1u. At these velocities, μ depends linearly on v. Only at $v > 0.01$, we observe shear-thinning. Just as in system 2, shear-

thinning in system 2u is caused by shear-alignment of the polymers resulting from the shear stress imposed by the solvent of which the velocity-gradient penetrates into the brush. The μ of system 3u is approx. 50% of μ for system 2u, because of slip at the interface.
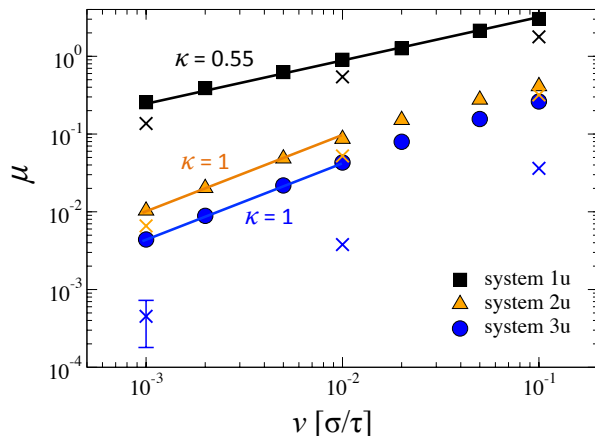
Figure 7: Friction coefficient μ versus velocity v upon shearing the undersaturated system 1u (black squares, fully miscible, no preferred absorbance), 2u (orange triangles, miscible solvents, preferred absorbance) and 3u (blue circles, immiscible solvents, preferred absorbance). The colored crosses denote μ for the same systems, but with immiscible polymers instead of the default miscible polymers employed in systems 1u-3u. The straight lines are fits to the power law relation $\mu = v^{\kappa}$.

The crosses in Figure 7 denote the friction coefficients for sliding systems 1u-3u using purely repulsive interactions between the polymers ($r_{\text{cut}} = 2^{1/6}\sigma_{\text{pp}}$), instead of the attractive interactions ($r_{\text{cut}} = 1.6\sigma_{\text{pp}}$) that are employed in the default systems. The polymer-polymer interactions only slightly affect μ for systems 1u and 2u (max. factor 2). However, for system 3u, polymer-immiscibility strongly affects the friction coefficient upon sliding the immiscible brush systems. The friction is more than 10 times lower for the immiscible polymers compared to the miscible polymers. A similar effect is observed for dry brushes, as we will discuss in the next paragraph. This strong effect of the polymer-miscibility on the friction is caused by decreased shear stress due to increased slip at the interface.

Dry brushes

Figure 8 shows snapshots of simulation cells in which we removed all the solvent such that the brushes are dry. These systems are equivalent to polymer brushes in poor solvent conditions, except for a potential viscous drag contribution upon relative sliding. However, the latter is expected to be small, due to the low-viscosity solvents that are generally employed. In contrast to solvated polymer brush systems, interdigitation in dry brushes strongly depends on the (im-)miscibility of the polymers. As for contacting bulk polymer films,[57] a small mismatch in the interaction-parameters strongly affects the overlap of the polymers across the interface. The brushes interdigitate for interaction-strengths $\varepsilon_{P\overline{P}}$ between polymers P and $\overline{P}$ that are equal or stronger than the interaction between polymers within the brush (ε_{PP} and $\varepsilon_{\overline{PP}}$). For $\varepsilon_{P\overline{P}} < \varepsilon_{PP}$ & $\varepsilon_{\overline{PP}}$ there is a smooth interface between the brushes.
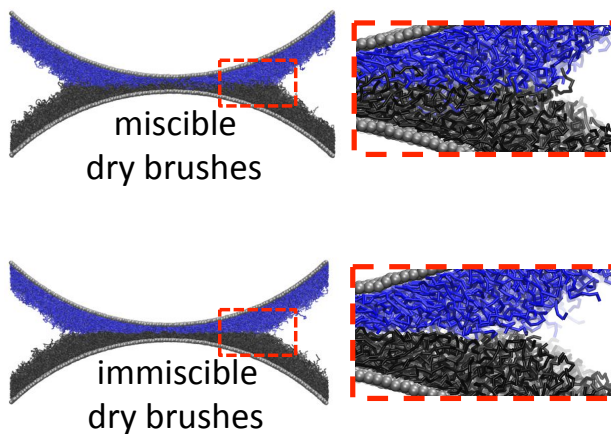
Figure 8: Simulation snapshots of contacting, dry, miscible (top) and immiscible (bottom) polymer brushes. The snapshots on the right are magnifications of the central region of the contact.

Figure 9 shows the friction coefficient μ versus velocity v upon sliding the dry, miscible (black squares) and immiscible (blue circles) brushes of Figure 8 at a normal load of $F_N = 4500\varepsilon/\sigma$. In agreement with experimental observations,[55,58,59] the friction coefficients for the miscible polymer brushes under dry or poor solvent conditions are larger than for fully-immersed swollen miscible systems. These results seem to disagree with former MD simulations,[60] in which was found that the friction for sliding miscible brushes in good solvent is higher than for miscible bushes in poor

15

solvent conditions. However, these simulations were performed in a parallel-plate geometry and consequently the solvent was forced to remain between the collapsed brushes under poor solvent conditions. In the experiments, where a sphere is pressed onto a flat surface[55,58,59] and in our simulations, the solvent flows out of the contact under poor solvent conditions leading to direct brush-brush contact, which results in much larger friction.
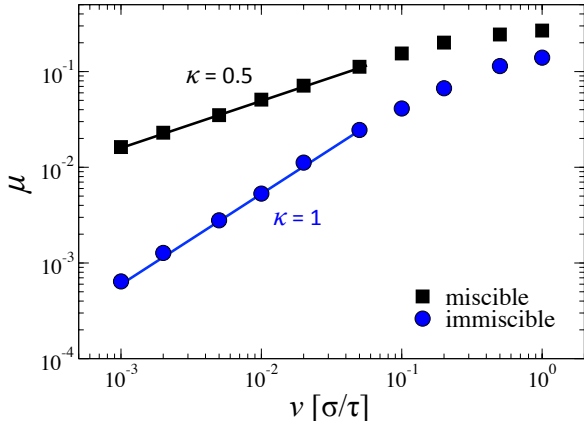
Figure 9: Friction coefficient μ versus velocity v upon shearing dry, miscible (black squares) and immiscible (blue circles) brushes. The straight lines are fits to the power law relation $\mu = v^\kappa$.

Figure 9 also shows that for the miscible systems at small velocities we find a power law scaling with shear-thinning exponent $\kappa = 0.5$. As expected, shear-thinning correlates with the decrease in the binary interaction count with increasing velocity. However, our exponent is smaller than the theoretically predicted exponent $\kappa = 0.69$ for dry brushes[19] and also smaller than the exponent $\kappa = 0.6$ observed for simulations in a parallel-plate geometry.[18] Our exponent of $\kappa = 0.5$ might be an effect of the geometry. For higher shear-rates polymers tilt in the direction of motion, but also move transverse to the direction of motion out of the contact. This results in a stronger decrease in overlap with increasing velocity than for the parallel plate geometry. The latter can result in a shear-thinning exponent that is lower than $\kappa = 0.69$. An alternative explanation can be that our dry brushes behave like polymer melts for which the shear-thinning exponent is close to $\kappa = 0.5$.[61,62] For the immiscible polymer brushes we find a linear relation between friction and velocity for small velocities. Only at velocities higher than $v = 0.1\sigma/\tau$ the immiscible brushes start to shear-

16

thin. At these velocities the binary interaction is still independent of the velocity. However, the overlap-integral[18] slightly decreases with increasing velocities. This implies that long-wavelength fluctuations of the interface between the brushes are smearing out and flattened at higher velocities. Moreover, the average distance between the brushes slightly increases with increasing velocity. The latter is consistent with MD simulations of immiscible polymer films in which shear thinning was found to correlate with a reduction in the radius of gyration of the polymers in the normal direction.[62]

Due to the different exponents for miscible and immiscible dry brushes, the difference in friction increases strongly with decreasing velocity. At the lowest velocity ($v = 0.001\sigma/\tau$) the friction for the immiscible brushes is approximately 5% of the friction for the miscible brushes. Experimentally, however, only small differences in the friction for dry, miscible and immiscible polymer brushes have been found.[23,63,64] Moreover, the experimentally measured friction force for sliding brushes in poor solvent conditions has been found to be almost independent of the velocity.[59,65] Both experimental observations we observe only at the higher sliding velocities ($v > 0.1\sigma/\tau$), which translate to velocities >70 cm/s. Experimental sliding velocities often do not exceed 100 μm/s. One possible explanation for this apparent discrepancy is that simulations and experiments have different Weissenberg numbers W (shear rate times the relaxation time of interdigitation). The relaxation time of the evolution of the density profile of a dry polystyrene brush that is brought into contact with a chemically identical network was found to be more than 10^4 s (3-4 hours),[66] while the typical shear rate at low velocities in AFM experiments is approximately 100 s^{-1}.[23,65] This means that AFM experiments of sliding dry brushes are performed at $W = 10^6$. In our simulations the relaxation time for interdigitation (determined from the long-time relaxation of the binary interaction count after switching the P$\bar{\text{P}}$ interactions from repulsive to attractive) $\tau_{\text{int}} \approx 10^4\tau$, while our shear-rate at the highest velocities is on the order of 1 τ^{-1}. This means that our simulations of sliding dry brushes are performed at $W = 10^4$ and, thus, that W for dry brush experiments at low velocities is approximately two orders of magnitude higher than W at the highest velocities of our simulations. Figure 9 shows indeed that at the highest velocities the friction tends to become inde-

pendent of the velocity and that the difference in friction between miscible and immiscible brushes at the velocities disappears. These tendencies are in line with the relations found in experiments performed at higher W.[23,59,63,65]

Conclusions

We discussed the effect of the solvation-method and of the miscibility of the different system-components on the measured friction coefficient for polymer brushes on curved surfaces. Within the range of velocities studied in this article, the largest difference in friction between miscible and immiscible polymer brush systems is found for the partially solvated systems. The friction for the miscible partially solvated system is high due to more direct polymer-polymer interactions and due the formed capillary that bundles the polymers together causing an tilting of the polymers towards the contact. In contrast, the polymers of the solvent-immersed miscible system show an outward polymer tilting due to the curvature of the surfaces. Consequently, there can be minimal interdigitation such that we observe a much lower friction compared to the undersaturated system. Nevertheless, in all studied brush-compositions, the friction for miscible polymer brush systems is higher than for immiscible systems. For the brushes that are fully immersed in the solvent, immiscibility of the polymer brush systems is mainly determined by the preferred absorbance of two solvents in the two different, opposing brushes. Therefore, the method still works for mixing solvents, as long as they demix in the contact. Moreover, as can be expected due to the effective repulsion for polymers in good solvent, the miscibility of the polymers have little to no effect on the frictional response. However, for systems where the brushes are undersaturated in solvent, the miscibility of the polymers more strongly affects the friction during relative sliding motion, because there is less solvent available to circumvent direct polymer-polymer contact. Especially, for the solvent-undersaturated, immiscible polymer brush system, the effect of polymer-miscibility on the friction coefficient is strong and almost comparable to the effect of polymer-miscibility in dry brushes.

Acknowledgement

References

(1) Wilkins, J. *Nature* **1968**, *219*, 1050.

(2) Jones, E. *Lancet* **1934**, *223*, 1426.

(3) McCutchen, C. W. *Wear* **1962**, *5*, 1.

(4) Klein, J.; Kumacheva, E.; Mahalu, D.; Perahia, D.; Fetters, L. J. *Nature* **1994**, *370*, 634.

(5) Moro, T.; Takatori, Y.; Ishihara, K.; Konno, T.; Takigawa, Y.; Matsushita, T.; Chung, U.-I.; Nakamura, K.; Kawaguchi, H. *Nature Mater.* **2004**, *3*, 829.

(6) Milner, S. T.; Witten, T. A.; Cates, M. E. *Macromolecules* **1988**, *21*, 2610.

(7) Cohen Stuart, M. A.; Huck, W. T. S.; Genzer, J.; Müller, M.; Ober, C.; Stamm, M.; Sukhorukov, G. B.; Szleifer, I.; Tsukruk, V. V.; Urban, M.; Winnik, F.; Zauscher, S.; Luzinov, I.; Minko, S. *Nature Mater.* **2010**, *9*, 101.

(8) Mendes, P. M. *Chem. Soc. Rev.* **2008**, *37*, 2512.

(9) Stanislav, J. F. *Rheol. Acta* **1982**, *565*, 564.

(10) Klein, J. *Annu. Rev. Mater. Sci.* **1996**, *26*, 581.

(11) Léger, L.; Raphaël, E.; Hervet, H. *Advances in Polymer Science* **1999**, *138*, 185.

(12) Binder, K.; Kreer, T.; Milchev, A. *Soft Matter* **2011**, *7*, 7159.

(13) Maeda, N.; Chen, N.; Tirrell, M.; Israelachvili, J. N. *Science* **2002**, *297*, 379.

(14) Bureau, L.; Léger, L. *Langmuir* **2004**, *20*, 4523.

(15) Goujon, F.; Malfreyt, P.; Tildesley, D. J. *Soft Matter* **2010**, *6*, 3472.

(16) Murat, M.; Grest, G. S. *Phys. Rev. Lett.* **1989**, *63*, 1074.

(17) Grest, G. S. *Phys. Rev. Lett.* **1996**, *76*, 4979.

(18) Kreer, T.; Müser, M. H.; Binder, K.; Klein, J. *Langmuir* **2001**, *17*, 7804.

(19) Galuschko, A.; Spirin, L.; Kreer, T.; Johner, A.; Pastorino, C.; Wittmer, J.; Baschnagel, J. *Langmuir* **2010**, *26*, 6418.

(20) Spirin, L.; Galuschko, A.; Kreer, T.; Johner, A.; Baschnagel, J.; Binder, K. *Eur. Phys. J. E* **2010**, *33*, 307.

(21) de Beer, S. *Langmuir* **2014**, *30*, 8085.

(22) Drummond, C. *Phys. Rev. Lett.* **2012**, *109*, 154302.

(23) de Beer, S.; Kutnyanszky, E.; Schön, P. M.; Vancso, G. J.; Müser, M. H. *Nat. Commun.* **2014**, *5*, 3781.

(24) de Beer, S.; Müser, M. H. *Soft Matter* **2013**, *9*, 7234.

(25) Persson, B. N. J.; Albohr, O.; Tartaglino, U.; Volokitin, A. I.; Tosatti, E. *J. Phys.: Condens. Matt.* **2005**, *17*, R1.

(26) Nommensen, P. A.; Duits, M. H. G.; van den Ende, D.; Mellema, J. *Phys. Rev. E* **1999**, *59*, 3147.

(27) Singh, S. P.; Winkler, R. G.; Gompper, G. *Phys. Rev. Lett.* **2011**, *107*, 158301.

(28) Briels, W. J. *Soft Matter* **2009**, *5*, 4401.

(29) Riedo, E.; Lévy, F.; Brune, H. *Phys. Rev. Lett.* **2002**, *88*, 185505.

(30) Lo Verso, F.; Yelash, L.; Egorov, S. A.; Binder, K. *J. Chem. Phys.* **2011**, *135*, 214902.

(31) Alexander, S. *J. Phys.-Paris* **1977**, *38*, 983.

(32) de Gennes, P. G. *Macromolecules* **1980**, *13*, 1069.

(33) Binder, K.; Milchev, A. *J. Polym. Sci. Part B: Polym. Phys.* **2012**, *50*, 1515.

(34) Murat, M.; Grest, G. S. *Macromolecules* **1991**, *24*, 704.

(35) Humphrey, W.; Dalke, A.; Schulten, K. *J. Molec. Graphics* **1996**, *14*, 33.

(36) Grest, G. S.; Kremer, K. *Phys. Rev. A* **1986**, *33*, 3628.

(37) He, G.; Müser, M. H.; Robbins, M. O. *Science* **1999**, *284*, 1650.

(38) Priezjev, N. V.; Troian, S. M. *Phys. Rev. Lett.* **2004**, *92*, 018302.

(39) Kremer, K.; Grest, G. S. *J. Chem. Phys.* **1990**, *92*, 5057.

(40) Descas, R.; Sommer, J.-U.; Blumen, A. *Macromol. Theory Simul.* **2008**, *17*, 429.

(41) Ingebrigsten, T.; Toxvaerd, S. *J. Phys. Chem. C* **2007**, *111*, 8518.

(42) Plimpton, S. *J. Comp. Phys.* **1995**, *117*, 1.

(43) Thompson, P. A.; Robbins, M. O. *Phys. Rev. A* **1990**, *41*, 6830.

(44) Wang, N.; Trunfio-Sfarghiu, A.-M.; Portinha, D.; Descartes, S.; Fleury, E.; Berthier, Y.; Rieu, J.-P. *Colloids Surf. B* **2013**, *108*, 285.

(45) Ramakrishna, S.; Espinosa-Marzal, R. M.; Naik, V. V.; Nalam, P. C.; Spencer, N. D. *Langmuir* **2013**, *29*, 15251.

(46) Persson, B. N. J. *J. Phys. Chem.* **2001**, *115*, 3840.

(47) Magda, J. J.; Fredrickson, G. H.; Larson, R. G.; Helfand, E. *Macromolecules* **1988**, *21*, 726.

(48) Winnink, F. M.; Ringsdorf, H.; Venzmer, J. *Macromolecules* **1990**, *23*, 2415.

(49) Mukherji, D.; Kremer, K. *Macromolecules* **2013**, *46*, 9158.

(50) Auroy, P.; Auvray, L. *Macromolecules* **1992**, *25*, 4134.

(51) Marko, J. F. *Macromolecules* **1993**, *26*, 313.

(52) Spirin, L.; Kreer, T. *ACS Macro Lett.* **2013**, *2*, 63.

(53) Koplik, J.; Banavar, J. R. *Phys. Rev. Lett.* **2006**, *96*, 044505.

(54) Müller, M. T.; Yan, X.; Lee, S.; Perry, S. S.; Spencer, N. D. *Macromolecules* **2005**, *38*, 5706.

(55) Kobayashi, M.; Terayama, Y.; Hosaka, N.; Kaido, M.; Suzuki, A.; Yamada, N.; Torikai, N.; Ishihara, K.; Takahara, A. *Soft Matter* **2007**, *3*, 740.

(56) Biesalski, M.; Johannsmann, D.; Rühe, J. *Macromol. Symp.* **1999**, *145*, 113.

(57) Ge, T.; Grest, G. S.; Robbins, M. O. *ACS Macro Lett.* **2013**, *2*, 882.

(58) Schorr, P. A.; Kwan, T. C. B.; Kilbey, S. M.; Shaqfeh, E. S. G.; Tirrell, M. *Macromolecules* **2003**, *36*, 389.

(59) Nomura, A.; Okayasu, K.; Ohno, K.; Fukuda, T.; Tsujii, Y. *Macromolecules* **2011**, *44*, 5013.

(60) Goujon, F.; Malfreyt, P.; Tildesley, D. J. *Macromolecules* **2009**, *42*, 4310.

(61) Xu, Z.; de Pablo, J. J.; Kim, S. *J. Chem. Phys.* **1995**, *102*, 5836.

(62) Barsky, S.; Robbins, M. O. *Phys. Rev. E* **2002**, *65*, 021808.

(63) Vyas, M. K.; Schneider, K.; Nandan, B.; Stamm, M. *Soft Matter* **2008**, *4*, 1024.

(64) Zeng, H.; Tian, Y.; Zhao, B.; Tirrell, M.; Israelachvili, J. *Langmuir* **2009**, *25*, 4954.

(65) Espinosa-Marzal, R. M.; Bielecki, R. M.; Spencer, N. D. *Soft Matter* **2013**, *9*, 10572.

(66) Geoghegan, M.; Clarke, C. J.; Boué, F.; Menelle, A.; Russ, T.; Bucknall, D. G. *Macro-molecules* **1999**, *32*, 5106.

Graphical TOC Entry

transverse
polymer tilting:

escaping
INTERDIGITATION